Theoretical analysis of simply supported channel girder bridges

Hong-Song Hu[*1], Jian-Guo Nie[2] and Yu-Hang Wang[3]

[1]*Disaster Prevention Research Institute (DPRI), Kyoto University, Gokasho, Uji, Kyoto 611-0011, Japan*
[2]*Department of Civil Engineering, Tsinghua University, Beijing 100084, China*
[3]*School of Civil Engineering, Chongqing University, Chongqing 400045, China*

Abstract.   Channel girder bridges that consist of a deck slab and two side beams are good choices for railway bridges and urban rail transit bridges when the vertical clearance beneath the bridge is restricted. In this study, the behavior of simply supported channel girder bridges was theoretical studied based on the theory of elasticity. The accuracy of the theoretical solutions was verified by the finite element analysis. The global bending of the channel girder and the local bending of the deck slab are two contributors to the deformations and stresses of the channel girder. Because of the shear lag effect, the maximum deflection due to the global bending could be amplified by 1.0 to 1.2 times, and the effective width of the deck slab for determining the global bending stresses can be as small as 0.7 of the actual width depending on the width-to-span ratio of the channel girder. The maximum deflection and transversal stress due to the local bending are obtained at the girder ends. For the channel girders with open section side beams, the side beam twist has a negligible effect on the deflections and stresses of the channel girder. Simplified equations were also developed for calculating the maximum deformations and stresses.

Keywords: channel girder bridge; theoretical analysis; global bending; local bending; design equations

1. Introduction

The channel girder bridge is a relatively new type of girder bridge. It is a good choice for railway bridges and urban rail transit bridges when the vertical clearance beneath the bridge is restricted. The concept of channel girder bridge was developed mainly in the early 1990s when several examples of channel girder bridges were built in Europe (Shepherd and Gibbens 2004, Staquet *et al*. 2004). In the mid-1990s, the Highway Innovative Technology Evaluation Center of U.S. carried out a research program and built several channel girder bridges in the New York State (HITEC 1996). During the period of 2001 to 2003, the Sorell Causeway Bridge (Gibbens and Smith 2004) was built in Australia, which shall be the most famous channel girder bridge around the world. In recent years, a number of channel girder bridges have also been built in China, such as the Geshui Creek Railway Bridge (Zhu 1996), Jianghan Line Qinglong Bridge (Hu 2004), etc.

The channel girder bridge consists of a deck slab and two side beams, as shown in Fig. 1. The deck slab and side beams are posttensioned using longitudinal tendons which are anchored at the

---

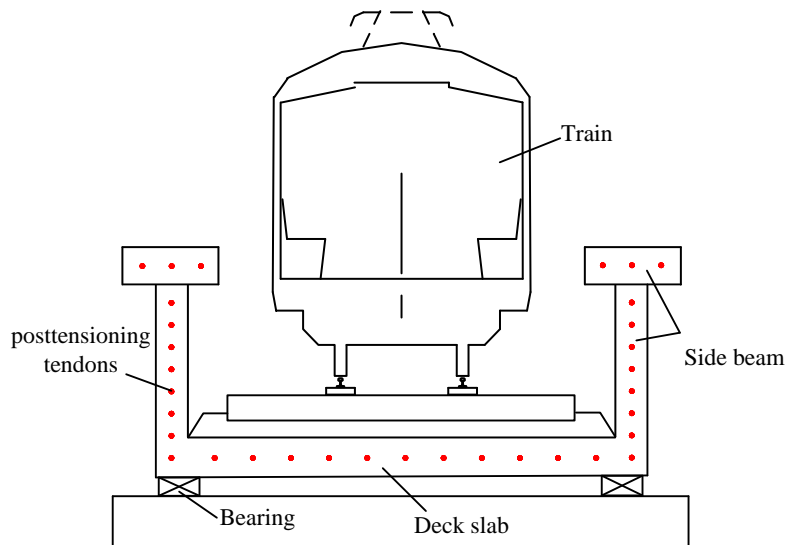∗Corresponding author, Ph.D., E-mail: hhsong05@gmail.com

Fig. 1 Configuration of the channel girder bridge

girder ends. Vertical and transversal posttensioning tendons may also be needed for the side beams and deck slab, respectively, to prevent the concrete cracking. Traffic moves on the deck slab, so besides taking part in the global longitudinal bending of the channel girder, the deck slab itself will bend in two directions (Li *et al*. 2011, Xiong *et al*. 2014). Because of the transversal bending of the deck slab, the side beams will twist in the section plane, which will in turn affect the local bending of the deck slab. When the width-to-span ratio of the channel girder is large, the shear lag effect (Gara *et al*. 2011, Zhou *et al*. 2011, Chen *et al*. 2014) may also have a great effect on the deflections and stresses of the channel girder.

Because of the complicated spatial behavior of the channel girder bridge, three-dimensional finite element analysis was usually conducted to calculate the deformations and stresses of the channel girder (Raju and Menon 2011, Raju and Menon 2013, Wu *et al*. 2013). Although the finite element analysis can provide accurate results, it is not favorable for understanding the general behavior of the channel girder, and for developing general design equations. In this study, the behavior of simply supported channel girders was theoretical studied using the theory of elasticity. Based on the theoretical solutions, simplified equations were also developed for calculating the maximum deformations and stresses.

2. Theoretical solutions

The theoretical derivations are based on the theory of elasticity (Timoshenko and Goodier 1970). The channel girder is assumed to be composed of a homogeneous and isotropic material. The side beams and deck slab can be regarded as "slender beam" and "thin plate", respectively, according to the general configurations of channel girders, i.e., the shear deformations of the side beams and deck slab can be neglected. The channel girder is simply supported at the four corners, and the external loads are assumed to be uniformly distributed on the surface of the deck slab. The coordinate system and sectional dimensions of the channel girder are shown in Fig. 2. The origin
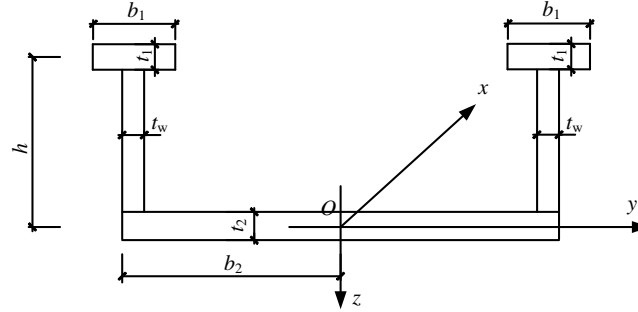
Fig. 2 Cross section and coordinate system of the channel girder

of coordinates locates in the deck slab center of one end cross section. The x, y, and z axis are in the longitudinal, transversal and vertical directions, respectively. Each side beam consists of a top flange and a web. As shown in Fig. 2, b_1 and t_1 are the width and thickness of the top flange, respectively; b_2 and t_2 are the half width and thickness of the deck slab, respectively; h is the distance between the center of the top flange and that of the deck slab, and t_w is the thickness of the web.

2.1 Deformation analysis

The deflections of the channel girder under vertical loads stem from the global bending of the channel girder and also the local bending of the deck slab, as shown in Fig. 3. Since the external loads are symmetrical about the longitudinal axis, the deflection due to the global bending can be denoted as $w_0(x)$, which doesn't vary in the transversal direction. The deflection due to the local bending of the deck slab $w_l(x,y)$, is assumed as (Timoshenko and Woinowsky-Krieger 1959)

$$w_l\left(x,y\right)=\left(\cos\frac{\pi y}{2b_2}\right)w_1\left(x\right) \tag{1}$$

where $w_1(x)$ needs to be determined. Therefore, the total deflection of the deck slab, $w_s(x,y)$, is

$$w_s\left(x,y\right)=w_0\left(x\right)+w_l\left(x,y\right)=w_0\left(x\right)+\left(\cos\frac{\pi y}{2b_2}\right)w_1\left(x\right) \tag{2}$$

The longitudinal displacement of the deck slab is assumed parabolically distributed along the slab width due to the shear lag effect (Gjelsvik 1991), so the longitudinal displacement at the mid-surface of the deck slab, $u_s(x,y)$, can be written as

$$u_s\left(x,y\right)=u_0\left(x\right)+\left(1-\frac{y^2}{b_2^2}\right)u_1\left(x\right) \tag{3}$$

where $u_0(x)$ is the longitudinal displacement at the intersection of the side beam and the mid-surface of the deck slab, and $u_1(x)$ is the maximum variation of the parabolic distribution.

The side beams will twist due to the transversal bending of the deck slab, as shown in Fig. 3(b). The twist angle of the side beams, $\theta(x)$, can be determined as
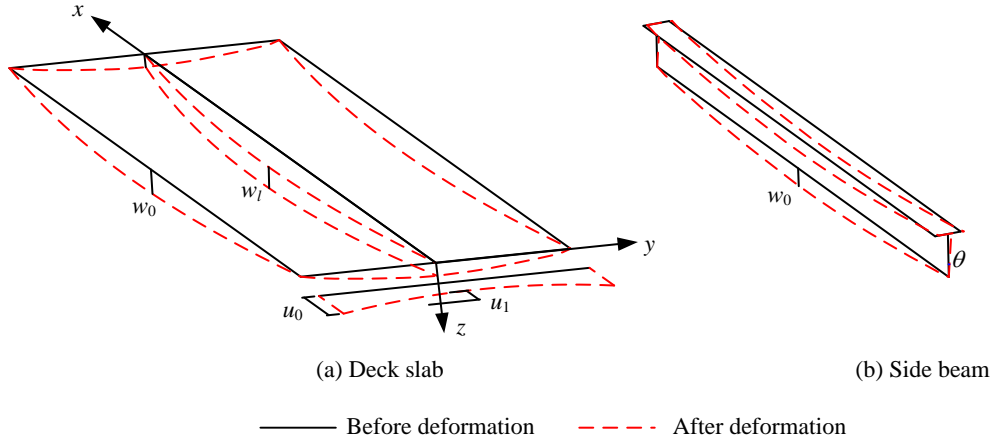
(a) Deck slab (b) Side beam

——— Before deformation — – — – After deformation

Fig. 3 Deformations of the channel girder

$$\theta(x) = \frac{\partial w_l}{\partial y}\bigg|_{y=b_2} = \frac{-\pi}{2b_2} w_1(x) \tag{4}$$

2.2 Strains and stresses

The longitudinal strain of the side beams, ε_{xb}, is

$$\varepsilon_{xb} = -w_0'' z + u_0' \tag{5}$$

and the corresponding longitudinal stress, σ_{xb}, is

$$\sigma_{xb} = E\varepsilon_{xb} = E(-w_0'' z + u_0') \tag{6}$$

where E is the elastic modulus. The longitudinal strain, ε_{xs1}, and transversal strain, ε_{ys1}, of the deck slab due to the global bending are

$$\varepsilon_{xs1} = \frac{\partial u_s}{\partial x} - \frac{\partial^2 w_0}{\partial x^2} z = u_0' + (1 - \frac{y^2}{b_2^2})u_1' - w_0'' z \tag{7}$$

$$\varepsilon_{ys1} = -\mu\varepsilon_{xs1} = -\mu\left(u_0' + (1 - \frac{y^2}{b_2^2})u_1' - w_0'' z\right) \tag{8}$$

where μ is the Poisson's ratio. The longitudinal strain, ε_{xs2}, and transversal strain, ε_{ys2}, of the deck slab due to the local bending are

$$\varepsilon_{xs2} = -\frac{\partial^2 w_l}{\partial x^2} z = -\left(\cos\frac{\pi y}{2b_2}\right)w_1'' z \tag{9}$$

$$\varepsilon_{ys2} = -\frac{\partial^2 w_l}{\partial y^2} z = \frac{\pi^2}{4b_2^2}\left(\cos\frac{\pi y}{2b_2}\right)w_1 z \tag{1}$$

Therefore, the total longitudinal strain, ε_{xs}, and transversal strain, ε_{ys}, of the deck slab are

$$\varepsilon_{xs} = \varepsilon_{xs1} + \varepsilon_{xs2} = u_0' + (1 - \frac{y^2}{b_2^2})u_1' - w_0''z - \left(\cos\frac{\pi y}{2b_2}\right)w_1''z \tag{11}$$

$$\varepsilon_{ys} = \varepsilon_{ys1} + \varepsilon_{ys2} = -\mu\left(u_0' + (1 - \frac{y^2}{b_2^2})u_1' - w_0''z\right) + \frac{\pi^2}{4b_2^2}\left(\cos\frac{\pi y}{2b_2}\right)w_1 z \tag{12}$$

The in-plane shear strain of the deck slab due to the local bending, γ_{xys1}, is

$$\gamma_{xys1} = -2\frac{\partial^2 w_l}{\partial x \partial y}z = \frac{\pi}{b_2}\left(\sin\frac{\pi y}{2b_2}\right)w_1'z \tag{13}$$

and the in-plane shear strain of the deck slab due to the shear lag effect, γ_{xys2}, is

$$\gamma_{xys2} = \frac{\partial u_s}{\partial y} = -\frac{2y}{b_2^2}u_1 \tag{14}$$

so the total in-plane shear strain of the deck slab, γ_{xys}, is

$$\gamma_{xys} = \gamma_{xys1} + \gamma_{xys2} = \frac{\pi}{b_2}\left(\sin\frac{\pi y}{2b_2}\right)w_1'z - \frac{2y}{b_2^2}u_1 \tag{15}$$

From the Hooke's Law, we can obtain each stress component of the deck slab:

$$\sigma_{xs} = \frac{E}{1-\mu^2}(\varepsilon_{xs} + \mu\varepsilon_{ys}) = E\left(u_0' + (1 - \frac{y^2}{b_2^2})u_1' - w_0''z\right) + \frac{E}{1-\mu^2}\left(-\left(\cos\frac{\pi y}{2b_2}\right)w_1''z + \mu\frac{\pi^2}{4b_2^2}\left(\cos\frac{\pi y}{2b_2}\right)w_1 z\right) \tag{16}$$

$$\sigma_{ys} = \frac{E}{1-\mu^2}(\varepsilon_{ys} + \mu\varepsilon_{xs}) = \frac{E}{1-\mu^2}\left(\frac{\pi^2}{4b_2^2}\left(\cos\frac{\pi y}{2b_2}\right)w_1 z - \mu\left(\cos\frac{\pi y}{2b_2}\right)w_1''z\right) \tag{17}$$

$$\tau_{xys} = G\gamma_{xys} = G\left(\frac{\pi}{b_2}\left(\sin\frac{\pi y}{2b_2}\right)w_1'z - \frac{2y}{b_2^2}u_1\right) \tag{18}$$

where σ_{xs}, σ_{ys} and τ_{xys} are the longitudinal, transversal and in-plane shear stresses of the deck slab, respectively, and G is the shear modulus of elasticity.

From the equilibrium of axial forces, we have

$$N = 2\int_{A_t+A_w}\sigma_{xb}dA + \int_{A_b}\sigma_{xs}dA = 2E\left(u_0'(A_t + A_w + \frac{1}{2}A_b) - w_0''(S_t + S_w) + \frac{1}{3}A_bu_1'\right) = 0 \tag{19}$$

where $A_t = b_1 t_1$, $A_w = (h - t_1/2 - t_2/2)t_w$ and $A_b = 2b_2 t_2$ are the sectional areas of each top flange, web and deck slab, respectively, and $S_t = -A_t h$ and $S_w = -A_w(h/2 - t_1/4 + t_2/4)$ are the moments of area of each top flange and web with respect to the y axis, respectively. Eq. (19) can be rewritten as

$$u_0' = -\frac{2A_b}{3A}u_1' + \frac{2(S_t + S_w)}{A}w_0'' = \alpha u_1' + z_c w_0'' \tag{20}$$

where $A=2(A_t+A_w)+A_b$ is the sectional area of the channel girder, $\alpha=-2A_b/3A$, and $z_c=2(S_t+S_w)/A$ represents the location of the neutral axis of the channel girder section without shear lag effect.

2.3 Determination of displacement functions

The variation principle (Washizu 1975) is used here to determine the three displacement functions, $w_0(x)$, $w_1(x)$, and $u_0(x)$. The strain energy of each side beam, U_1, is

$$U_1 = \int_0^l dx \int_{A_t+A_w} \frac{1}{2} E \varepsilon_{xb}^2 dA + \int_0^l \frac{1}{2} GI_t \theta'^2 dx$$

$$= \frac{1}{2} \int_0^l \left(E(I_{yt} + I_{yw} - (A_t + A_w + A_b)z_c^2)w_0''^2 + E(A_t + A_w)\alpha^2 u_1'^2 - EA_b \alpha z_c w_0'' u_1' \right) dx + \frac{1}{2} \int_0^l \frac{\pi^2}{4b_2^2} GI_t w_1'^2 dx$$

(21)

where $I_{yt} = b_1 t_1^3/12 + A_t h^2$ and $I_{yw} = t_w \left(h - t_1/2 - t_2/2 \right)^3/12 + A_w \left(h/2 - t_1/4 + t_2/4 \right)^2$ are the moments of inertia of each top flange and web with respect to the y axis, respectively, $I_t = b_1 t_1^3/3 + \left(h - t_1/2 - t_2/2 \right)t_w^3/3$ is the torsional moment of inertia of each side beam, and l is the span length of the channel girder. The strain energy of the deck slab, U_2, is

$$U_2 = 2\int_0^l dx \int_{\frac{1}{2}A_b} \frac{1}{2}(\sigma_{xs}\varepsilon_{xs} + \sigma_{ys}\varepsilon_{ys} + \tau_{xys}\gamma_{xys})dA$$

$$= \int_0^l (\frac{1}{2} E(I_{yb} + A_b z_c^2)w_0''^2 + \frac{4Gt_2}{3b_2}u_1^2 + (\frac{1}{2}\alpha^2 + \frac{2}{3}\alpha + \frac{4}{15})EA_b u_1'^2 + (\frac{2}{3} + \alpha)EA_b z_c w_0'' u_1' \qquad (22)$$

$$+ C_5 w_0'' w_1'' + C_6 w_1^2 + C_7 w_1'^2 + C_8 w_1''^2 + C_9 w_1 w_1'')dx$$

where $I_{yb} = b_2 t_2^3/6$ is the moment of inertia of the deck slab with respect to the y axis, $C_5 = 2EI_{yb}/\pi$, $C_6 = \pi^4 D_s/(32b_2^3)$, $C_7 = \pi^2 Gt_2^3/(24b_2) + \pi^2 GI_t/(4b_2^2)$, $C_8 = D_s b_2/2$, $C_9 = -\pi^2 \mu D_s/(4b_2)$, and $D_s = Et_2^3/(12(1-\mu^2))$ is the flexural stiffness of the deck slab. Therefore, the total strain energy of the channel girder, U, is

$$U = 2U_1 + U_2 = \int_0^l \left(C_1 w_0''^2 + C_2 u_1^2 + C_3 u_1'^2 + C_4 w_0'' u_1' + C_5 w_0'' w_1'' + C_6 w_1^2 + C_7 w_1'^2 + C_8 w_1''^2 + C_9 w_1 w_1'' \right)dx \quad (23)$$

where $C_1 = E(I_y - Az_c^2)/2$, $C_2 = 4Gt_2/(3b_2)$, $C_3 = (4/15 + \alpha/3)EA_b$, $C_4 = 2EA_b z_c/3$, and $I_y = 2I_{yt} + 2I_{yw} + I_{yb}$ is the moment of inertia of the channel girder with respect to the y axis.

The potential energy of the external loads, W, is

$$W = -\int_0^l dx \int_{-b_2}^{b_2} q(w_0 + \cos\frac{\pi y}{2b_2}w_1)dy = -\int_0^l 2qb_2(w_0 + \frac{2}{\pi}w_1)dx \qquad (24)$$

where q is the uniform surface load acting on the deck slab. So the total potential energy, Π, is

$$\Pi = U + W \qquad (25)$$

From the first variation of the total potential energy with respect to $w_0(x)$ equal to 0, we have

$$\begin{cases} 2C_1 w_0^{(4)} + C_4 u_1^{(3)} + C_5 w_1^{(4)} - 2qb_2 = 0 \\ \left(2C_1 w_0^{''} + C_4 u_1^{'} + C_5 w_1^{''} \right)\big|_{x=0,l} = 0 \\ w_0 \big|_{x=0,l} = 0 \end{cases} \tag{26}$$

Since C_5 is minute compared to C_1, and $w_0(x)$ and $w_1(x)$ are in the same order of magnitude, the terms of $w_1(x)$ in Eq. (26) can be omitted, and Eq. (26) can be simplified to

$$\begin{cases} 2C_1 w_0^{''} + C_4 u_1^{'} - qb_2 x(x-l) = 0 \\ w_0 \big|_{x=0,l} = 0 \end{cases} \tag{27}$$

From the first variation of the total potential energy with respect to $u_1(x)$ equal to 0, we have

$$\begin{cases} 2C_2 u_1 - 2C_3 u_1^{''} - C_4 w_0^{(3)} = 0 \\ \left(2C_3 u_1^{'} + C_4 w_0^{''} \right)\big|_{x=0,l} = 0 \end{cases} \tag{28}$$

The solutions for the system of differential equations composed of Eq. (27) and (28) are

$$u_1(x) = B_1 qb_2 \sinh\left(k_1 x\right) + B_2 qb_2 \cosh\left(k_1 x\right) + \frac{k_2}{k_1^2} qb_2 \left(2x - l\right) \tag{29}$$

$$w_0(x) = -\frac{C_4 qb_2}{2C_1 k_1}\left(B_2 \sinh\left(k_1 x\right) + B_1 \cosh\left(k_1 x\right)\right) + \frac{qb_2}{24C_1} x^4 - \frac{qb_2 l}{12C_1} x^3 - \frac{C_4 k_2 qb_2}{2C_1 k_1^2} x^2 + \left(\frac{qb_2 l^3}{24C_1} + \frac{C_4 k_2 qb_2 l}{2C_1 k_1^2}\right) x - \frac{C_4 k_2 qb_2}{C_1 k_1^4} \tag{30}$$

where $k_1 = \sqrt{4C_1 C_2 \big/ \left(4C_1 C_3 - C_4^2\right)}$, $k_2 = C_4 \big/ \left(4C_1 C_3 - C_4^2\right)$, $B_1 = -2k_2 \big/ k_1^3$, $B_2 = 2k_2 \left(\cosh(k_1 l) - 1\right)\big/\left(k_1^3 \sinh(k_1 l)\right)$.

From the first variation of the total potential energy with respect to $w_1(x)$ equal to 0, we have

$$\begin{cases} 2C_8 w_1^{(4)} + (2C_9 - 2C_7)w_1^{''} + 2C_6 w_1 + C_5 w_0^{(4)} - \dfrac{4qb_2}{\pi} = 0 \\ \left(-2C_8 w_1^{(3)} + (2C_7 - C_9)w_1^{'} - C_5 w_0^{(3)}\right)\big|_{x=0,l} = 0 \\ \left(2C_8 w_1^{''} + C_9 w_1 + C_5 w_0^{''}\right)\big|_{x=0,l} = 0 \end{cases} \tag{31}$$

Substituting the expressions of C_5 to C_9 into Eq. (31) gives

$$\begin{cases} w_1^{(4)} - 2(1+\beta)a^2 w_1^{''} + a^4 w_1 + \dfrac{4(1-\mu^2)}{\pi} w_0^{(4)} - \dfrac{4q}{\pi D_s} = 0 \\ \left(-w_1^{(3)} + (2+2\beta-\mu)a^2 w_1^{'} - \dfrac{4(1-\mu^2)}{\pi} w_0^{(3)}\right)\bigg|_{x=0,l} = 0 \\ \left(w_1^{''} - \mu a^2 w_1 + \dfrac{4(1-\mu^2)}{\pi} w_0^{''}\right)\bigg|_{x=0,l} = 0 \end{cases} \tag{32}$$
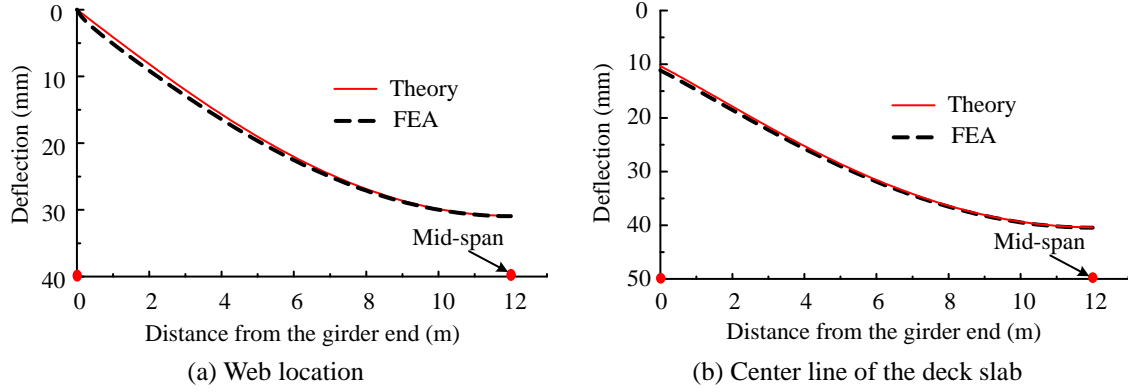
(a) Web location

(b) Center line of the deck slab

Fig. 4 Deflection along the longitudinal direction

(a) Transversal stress at the center line of the top surface of the deck slab

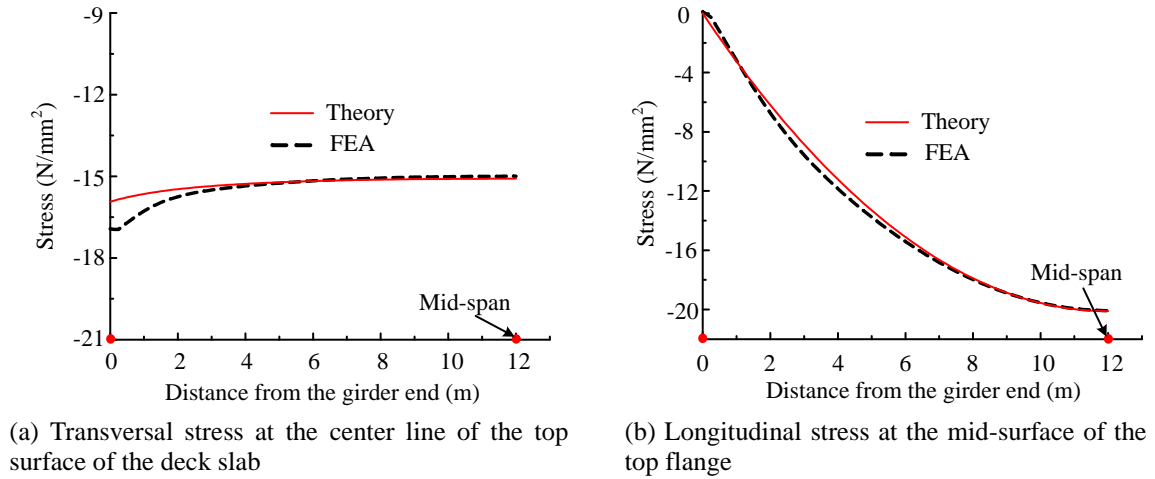(b) Longitudinal stress at the mid-surface of the top flange

Fig. 5 Stress distributions along the longitudinal direction

where $\beta = GI_t/Db_2$, $a = \pi/(2b_2)$. Solving the differential equation in Eq. (32) gives

$$w_1(x) = \frac{4(1-\mu^2)C_4 k_1^3 q b_2}{2\pi C_1\left(\left(a^2 - k_1^2\right)^2 - 2\beta a^2 k_1^2\right)}\left(B_1 \cosh(k_1 x) + B_2 \sinh(k_1 x)\right) - \frac{4(1-\mu^2) q b_2}{\pi C_1 a^4} + \frac{4q}{\pi D_s a^4}$$
$$+ D_1 \sinh(\beta_1 a x) + D_2 \cosh(\beta_1 a x) + D_3 \sinh(\beta_2 a x) + D_4 \cosh(\beta_2 a x) \tag{33}$$

where $\beta_1 = \sqrt{\beta + 1 + \sqrt{\beta(\beta+2)}}$, $\beta_2 = \sqrt{\beta + 1 - \sqrt{\beta(\beta+2)}}$, and D_1, D_2, D_3 and D_4 can be determined using the four boundary conditions in Eq. (32).

2.4 Verification

A prototype channel girder bridge (Xu 1984) built in Beijing is considered here for analysis. The sectional dimensions of the prototype bridge are as follows: $b_1 = 1000$ mm, $t_1 = 500$ mm,

(a) Transversal stress at the top surface of the deck slab

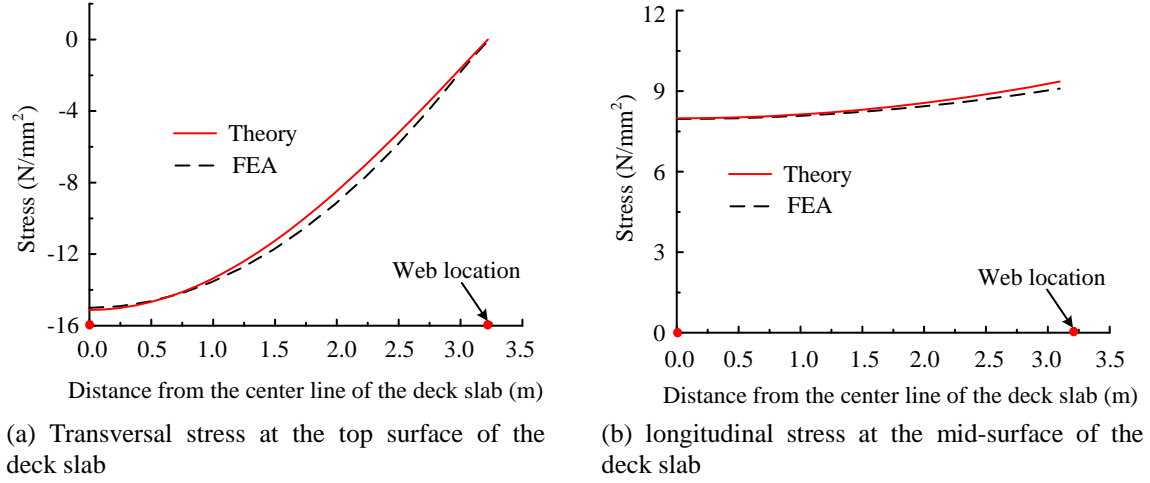(b) longitudinal stress at the mid-surface of the deck slab

Fig. 6 Stress distributions in the mid-span of the channel girder along the transversal direction

b_2=3220 mm, t_2=450 mm, h=1925 mm, and t_w=300 mm. The span length of the bridge, l, is 24 m, and the uniform surface load applied on the deck slab, q, is 100 kN/m². The elastic modulus and Poisson's ratio are taken as 30×10^3 N/mm² and 0.2, respectively.

Finite element analysis was conducted in the MSC.Mentat/Marc (2010) program (MSC.Software 2010) to verify the accuracy of the theoretical solutions. All the components of the channel girder were modeled using an eight-node thick shell element. The vertical displacements at the four corners were constrained to model the simply supported boundary conditions. Appropriate horizontal displacement constraints were also applied to eliminate the rigid body motions. As shown in Fig. 4 to Fig. 6, the deflections and stress components calculated from the theoretical solutions agree well with those from finite element analysis, so the derived equations can be used to analyze the behavior of the channel girder.

3. Behavior and design

3.1 Global bending

From Eq. (30), we know the maximum deflection due to the global bending is

$$w_0\left(l/2\right)=\frac{5qb_2l^4}{384C_1}+\frac{C_4k_2qb_2}{C_1k_1^2}\left(\frac{48l^2}{384}-\frac{1}{k_1^2}+\frac{1}{k_1^2\cosh\left(k_1l/2\right)}\right)=\zeta\frac{5qb_2l^4}{384C_1} \qquad (34)$$

where

$$\zeta=1+\frac{96C_4^2}{5C_1C_2l^2}\left(\frac{48}{384}-\frac{1}{k_1^2l^2}+\frac{1}{k_1^2l^2\cosh\left(k_1l/2\right)}\right) \qquad (35)$$

is referred to as the deflection amplification coefficient, and $5qb_2l^4/384C_1$ is the maximum deflection of a general beam subjected to uniformly distributed loads.

From Eq. (6) and (20), we have

$$\sigma_{xb} = E\left(\left(z_c - z\right)w_0'' + \alpha u_1'\right) \tag{36}$$

By taking σ_{xb} as zero, we can obtain the location of the neutral axis of the section including the shear lag effect:

$$z_{ce} = z_c + \frac{\alpha u_1'}{w_0''} \tag{37}$$

The contribution of the deck slab to the global bending can be expressed by the effective width coefficient, λ, i.e., the effective width of the deck slab is $\lambda(2b_2)$. Therefore, the location of the neutral axis of the equivalent section can be written as

$$z_{ce} = \frac{2\left(S_t + S_w\right)}{A + \left(\lambda - 1\right)A_b} = \frac{z_c A}{A + \left(\lambda - 1\right)A_b} \tag{38}$$

By combining Eq. (37) and (38), the formula for determining the effective width coefficient can be obtained:

$$\lambda = 1 - \frac{\alpha u_1'}{\alpha u_1' + w_0'' z_c} \frac{A}{A_b} \tag{39}$$

From Eq. (16) and (20), we know the longitudinal stress of the deck slab due to the global bending, σ_{xs1}, is

$$\sigma_{xs1} = E\left((\alpha + 1 - \frac{y^2}{b_2^2})u_1' + \left(z_c - z\right)w_0''\right) \tag{40}$$

The effective width coefficient can also be determined from

$$\lambda = \frac{\iint_{A_b} \sigma_{xs1} dA}{2b_2 \int_{-t_2/2}^{t_2/2} \sigma_{xs1}\big|_{y=b_2} dz} = 1 + \frac{2u_1'/3}{\alpha u_1' + z_c w_0''} \tag{41}$$

Eq. (39) and Eq. (41) are equivalent since $\alpha = -2A_b/3A$.

According to the general configurations of channel girder bridges, a series of channel girders were designed for the parametric study and numerical fitting. The half width of the deck slab, b_2, was fixed as 3000mm, and the values of h/b_2, t_2/b_2, t_w/t_2, t_1/t_2, b_1/t_w and l/b_2, were varied parametrically according to Table 1. In total, 3024 channel girders were obtained and analyzed.

Table 1 Values for each parameter

Parameter	Value
h/b_2	0.4, 0.6, 0.8, 1.0, 1.2, 1.4, 1.6
t_2/b_2	0.1, 0.15, 0.2, 0.25
t_w/t_2	0.5, 0.75, 1
t_1/t_2	1
b_1/t_w	1, 2, 3, 4
l/b_2	4, 6, 8, 10, 12, 14, 16, 18, 20

(a) ζ (b) $\lambda_{1/2}$
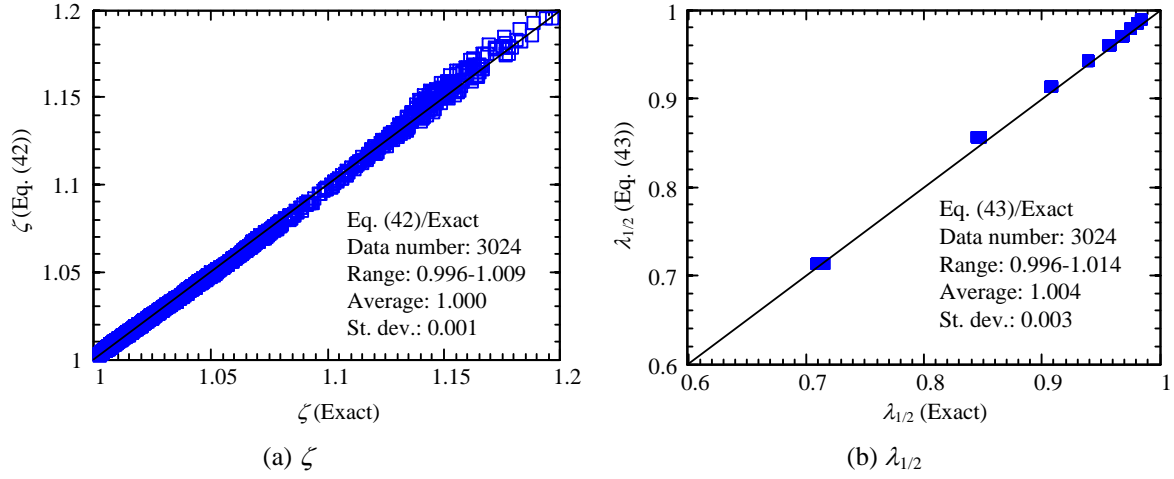
Fig. 7 Comparison between the exact solutions and simplified equations for ζ and $\lambda_{1/2}$

From the parametrical study, it was found that the deflection amplification coefficient, ζ, could be precisely determined from

$$\zeta = 1 + \frac{E}{G}\left(\frac{A_b z_c^2}{I_y - A z_c^2}\right)\left(2.6\left(\frac{b_2}{l}\right)^2 + 0.05\frac{b_2}{l}\right) \tag{42}$$

where $A_b z_c^2 / (I_y - A z_c^2)$ represents the ratio of the moment of inertia provided by the deck slab to the total moment of inertia of the channel girder section. The values of ζ are between 1.0 and 1.2, and increase as the values of $A_b z_c^2 / (I_y - A z_c^2)$ and b_2/l increase. The effective width coefficient at the mid-span, $\lambda_{1/2}$, mainly depends on the width-to-span ratio of the channel girder, $2b_2/l$, and can be calculated by

$$\lambda_{1/2} = \begin{cases} 1 & (b_2/l \leq 1/25) \\ -3(b_2/l)^2 - 0.48(b_2/l) + 1.02 & (b_2/l > 1/25) \end{cases} \tag{43}$$
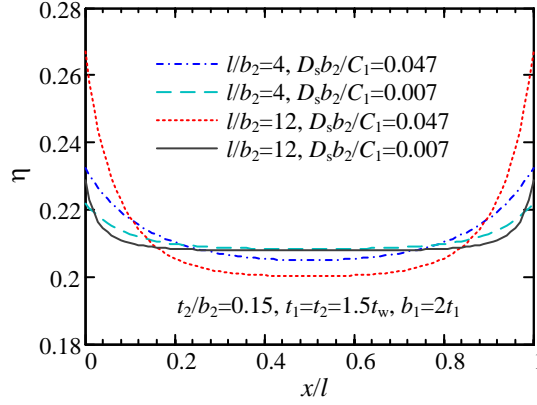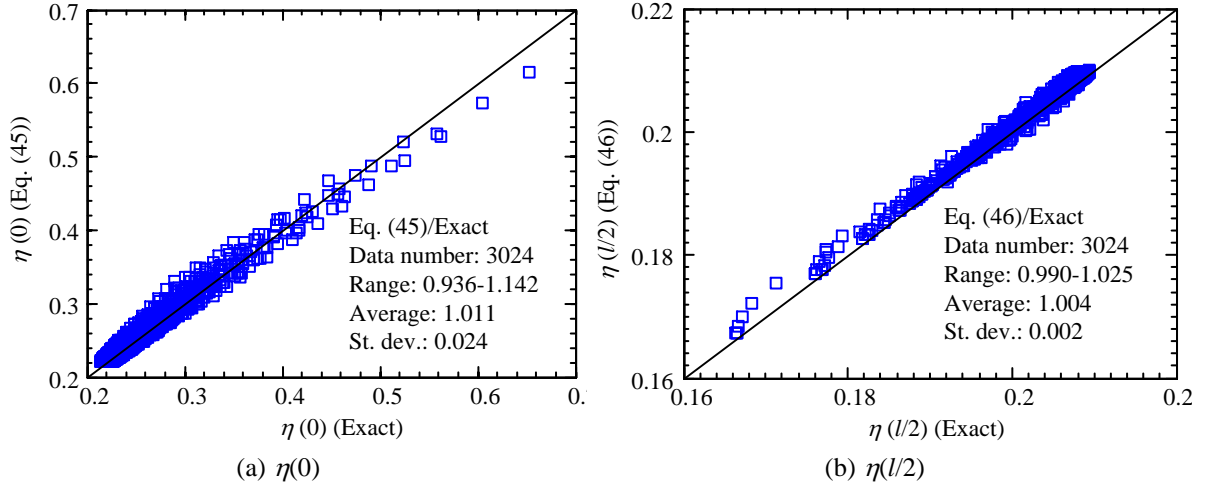
As shown in Fig. 7, the exact solutions and simplified equations for ζ and $\lambda_{1/2}$ are in good agreements.

3.2 Local bending

The deflection at the center line of the deck slab due to the local bending can be written as

$$w_1(x) = \eta(x)\frac{q b_2^4}{D_s} \tag{44}$$

where $\eta(x)$ was found mainly related to the width-to-span ratio of the channel girder, $2b_2/l$, and $D_s b_2/C_1$ which represents the ratio of the flexural stiffness of the deck slab to that of the channel

Fig. 8 Distribution of η along the girder span

(a) $\eta(0)$ (b) $\eta(l/2)$

Fig. 9 Comparison between the exact solutions and simplified equations for $\eta(0)$ and $\eta(l/2)$

girder. As shown in Fig. 8, the maximum value of $\eta(x)$ is obtained at the girder end, and the variation between the mid-span and girder end increases as the values of $D_s b_2/C_1$ and l/b_2 increase. From curve fitting analyses, accurate simplified equations were obtained for determining the values of $\eta(x)$ at the girder end and mid-span:

$$\eta(0) = \left(0.1 l/b_2 - 0.14\right)\frac{D_s b_2}{C_1} + 0.22 \tag{45}$$

$$\eta(l/2) = \begin{cases} \left(0.62\, b_2/l - 0.24\right)\dfrac{D_s b_2}{C_1} + 0.21 & \left(b_2/l > 1/15\right) \\[2mm] -0.2\dfrac{D_s b_2}{C_1} + 0.21 & \left(b_2/l \le 1/15\right) \end{cases} \tag{46}$$

As shown in Fig. 9, $\eta(l/2)$ ranges from 0.16 to 0.21, and is not sensitive to the configuration of the

channel girder, whereas $\eta(0)$ varies in a wider range, and can be up to 0.5 for large values of $D_s b_2/C_1$ and l/b_2.

From Eq. (16), we know the longitudinal stress of the deck slab due to the local bending, σ_{xs2}, is

$$\sigma_{xs2} = \frac{E}{1-\mu^2}\cos\frac{\pi y}{2b_2}\left(-w_1^{''} + \mu\frac{\pi^2}{4b_2^2}w_1\right)z \tag{47}$$

σ_{xs2} and the transversal stress of the deck slab, σ_{ys}, given by Eq. (17) can be written as

$$\sigma_{xs2} = \cos\frac{\pi y}{2b_2}\frac{12\left(\kappa_1(x)qb_2^2\right)}{t_2^3}z \tag{48}$$

$$\sigma_{ys} = \cos\frac{\pi y}{2b_2}\frac{12\left(\kappa_2(x)qb_2^2\right)}{t_2^3}z \tag{49}$$

where $\kappa_1(x)qb_2^2$ and $\kappa_2(x)qb_2^2$ are the bending moments at the center line of the deck slab due to the local bending. The coefficients, $\kappa_1(x)$ and $\kappa_2(x)$, are also mainly related to $D_s b_2/C_1$ and b_2/l. As shown in Fig. 10, the maximum value of $\kappa_1(x)$ is obtained at the mid-span, and that of $\kappa_2(x)$ is obtained at the girder end. Similar to the distribution of $\eta(x)$, $\kappa_2(x)$ is more uniformly distributed along the girder span for smaller values of $D_s b_2/C_1$ and l/b_2. From curve fitting analyses, simplified equations were obtained for determining the values of $\kappa_1(x)$ at the mid-span and $\kappa_2(x)$ at the girder end:

$$\kappa_1(l/2) = \begin{cases} (-0.4b_2/l - 0.067)\dfrac{D_s b_2}{C_1} + 0.103 & (b_2/l > 1/12) \\[3mm] -0.1\dfrac{D_s b_2}{C_1} + 0.103 & (b_2/l \leq 1/12) \end{cases} \tag{50}$$

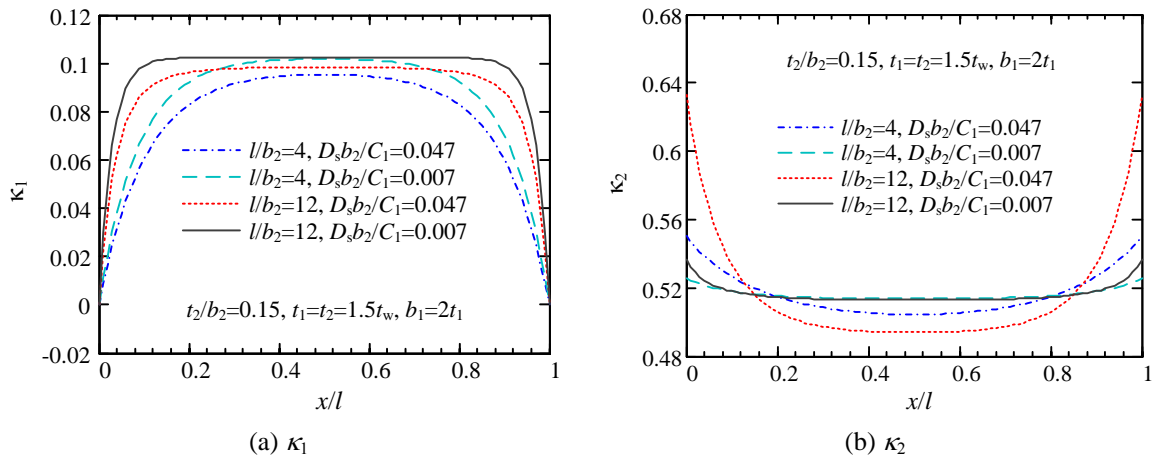$$\kappa_2(0) = (0.24l/b_2 - 0.34)\frac{D_s b_2}{C_1} + 0.51 \tag{51}$$

(a) κ_1 (b) κ_2

Fig. 10 Distributions of κ_1 and κ_2 along the girder span

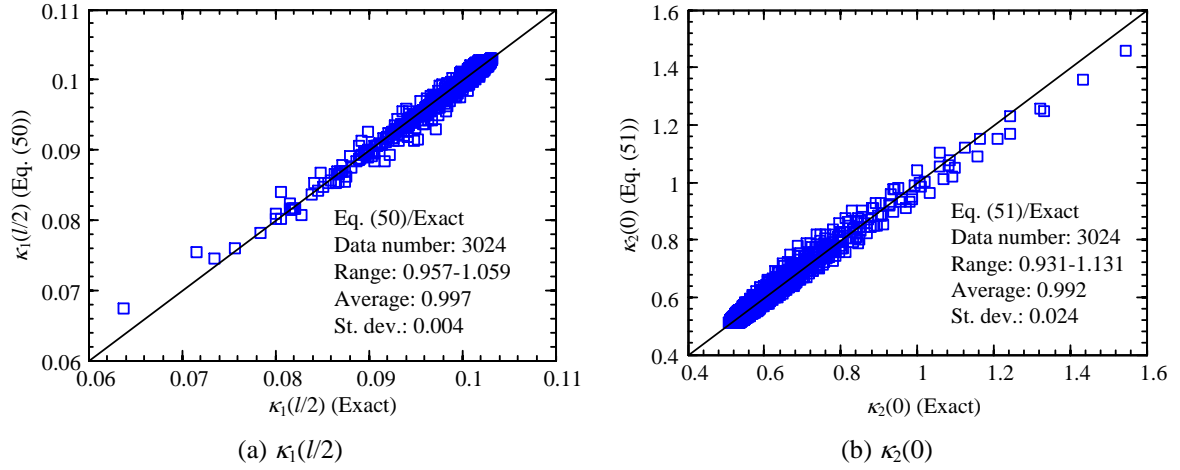(a) $\kappa_1(l/2)$ (b) $\kappa_2(0)$

Fig. 11 Comparison between the exact solutions and simplified equations for $\kappa_1(l/2)$ and $\kappa_2(0)$
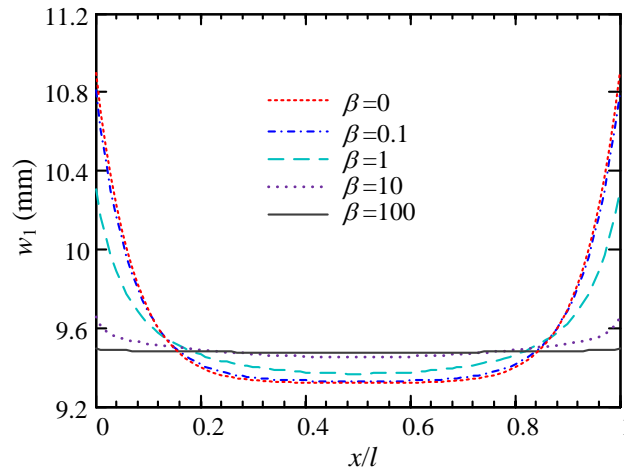

Fig. 12 Influence of β on $w_1(x)$ for the prototype bridge

Eq. (50) and (51) can give good predictions, as shown in Fig. 11.

$\beta=GI_t/Db_2$ in Eq. (32) reflects the ratio of the torsional stiffness of the side beam to the flexural stiffness of the deck slab. For the designed 3024 channel girders, the values of β are between 0.14 and 3.76. Larger values of β can be achieved through using box side beams. For the prototype bridge described in section 2.4, the influence of β on $w_1(x)$ is shown in Fig. 12. As the value of β increases, the distribution of $w_1(x)$ along the girder span becomes more uniform, since the large torsional stiffness of the side beam restrains the variation of twist angles, which is in direct proportion to $w_1(x)$ as given in Eq. (4). For the channel girders with open section side beams, the influence of the side beam twist is negligible.

4. Conclusions

A theoretical solution for simply supported channel girder bridges subjected to uniform surface loading was obtained based on the theory of elasticity and the variation principle. The global bending of the channel girder and the local bending of the deck slab are two contributors to the deformations and stresses of the channel girder. Because of the shear lag effect, the maximum deflection due to the global bending can be amplified by 1.0 to 1.2 times, and the amplification increases as the width-to-span ratio of the channel girder and the ratio of the moment of inertia provided by the deck slab to the total moment of inertia of the channel girder section increase. The effective width of the deck slab for calculating the global bending stresses is only dependent on the width-to-span ratio. The behavior of the local bending of the deck slab was mainly related to the width-to-span ratio and the ratio of the flexural stiffness of the deck slab to that of the channel girder. The maximum deflection and transversal stress due to the local bending are obtained at the girder ends. For the channel girders with open section side beams, the side beam twist has a negligible effect on the deflections and stresses of the channel girder.

Acknowledgements

References

Chen, J., Shen, S.L., Yin, Z.Y. and Horpibulsuk, S. (2014), "Closed-form solution for shear lag with derived flange deformation function", *J. Constr. Steel Res.*, **102**, 104-110.

Gara, F., Ranzi, G., and Leoni, G. (2011), "Simplified method of analysis accounting for shear-lag effects in composite bridge decks", *J. Constr. Steel Res.*, **67**(10), 1684-1697.

Gibbens, B., and Smith, P. S. (2004), "Design-construction of Sorell Causeway Channel Bridge, Hobart, Tasmania", *PCI J.*, **49**(3), 56-66.

Gjelsvik, A. (1991), "Analog-beam method for determining shear-lag effects", *J. Eng. Mech.*, **117**(7), 1575-1594.

Highway Innovative Technology Evaluation Center (HITEC) (1996), "Evaluation findings: the segmental concrete channel bridge system", CERF Reports HITEC 96-01.

Hu, C. (2004), "Construction technique of continuous trough girder of Jianghan Line Qinglong Bridge", *Rail. Stand. Des.*, **19**(6), 47-49. (in Chinese)

Li, R., Zhong, Y., Tian, B. and Du, J. (2011), "Exact bending solutions of orthotropic rectangular cantilever thin plates subjected to arbitrary loads", *Int. Appl. Mech.*, **47**(1), 107-119.

MSC Software (2010), "Marc 2010 volume A: Theory and user information", MSC Software Corporation.

Raju, V. and Menon, D. (2011), "Analysis of behaviour of U-girder bridge decks", *ACEE Int. J. Tran. Urban Devel.*, 1(1), 34-38.

Raju, V. and Menon, D. (2013), "Longitudinal analysis of concrete U-girder bridge decks", *Proceedings of the ICE-Bridge Engineering*, **167**(2), 99-110.

Shepherd, B. and Gibbens, B. (2004), "The evolution of the concrete "channel" bridge system and its application to road and rail bridges", *Fib Concrete Structures (Symposium)*, Avignon, France, April.

Staquet, S., Rigot, G., Detandt, H. and Espion, B. (2004), "Innovative composite precast prestressed

precambered U-shaped concrete deck for Belgium's high speed railway trains", *PCI J.*, **49**(6), 94-113.

Timoshenko, S.P. and Woinowsky-Krieger, S. (1959), *Theory of Plates and Shells*, McGraw-Hill, New York.

Timoshenko, S.P. and Goodier, J. N. (1970), *Theory of Elasticity* McGraw-Hill, New York.

Washizu, K. (1975), *Variational Methods in Elasticity and Plasticity*, 2nd Edition, Pergamon Press, Oxford.

Wu, L., Nie, J., Lu, J., Fan, J. and Cai, C.S. (2013), "A new type of steel-concrete composite channel girder and its preliminary experimental study", *J. Constr. Steel Res.*, **85**, 163-177.

Xiong, W., Cai, C.S., Ye, J. and Ma, Y. (2014), "Analytical solution on highway U-shape bridges using isotropic plate theory", *KSCE J. Civil Eng.*, 1-13.

Xu, Y. (1984), "Design of prestressed concrete trough girder bridges", *Rail. J.*, **6**(2), 82-89.

Zhu, H. (1996), "General design of continuous channel girder of Geshui Creek Railway Bridge", *Bridge Des.*, **10**(3), 49-51. (in Chinese)

Zhou, S. J. (2011), "Shear lag analysis in prestressed concrete box girders", *J. Bridge Eng.*, **16**(4), 500-512.

CC